Modeling of Convective Heat Transfer in the Liquid Core of the Earth

Modeling of Convective Heat Transfer in the Liquid Core of the Earth

S Solovjev[1], T M Popova[1]

[1]Department of Applied Mathematics, Pacific National University,
st. Tihookeanskaya 136, Khabarovsk, 680035, Russia

E-mail: solovjovsv@rambler.ru

Abstract. The results of numerical modeling of convective heat transfer of an electrically conductive liquid in a spherical layer are presented. The influence of the heat of Joule dissipation, the Grashof number and internal heat sources uniformly distributed in the liquid on the structure of the flow of an electrically conductive liquid, the temperature field, magnetic induction and the distribution of local Nusselt numbers are investigated when the vector acceleration of gravity is directed along the radius k the center of the spherical layer.

1. Introduction

The study of a wide class of problems of convective heat transfer of liquids in spherical concentration layers is of great importance, and in most cases the Boussinesq approximation is used in the fluid motion equation, in which the acceleration vector of free fall is directed vertically downwards. However, in a number of fundamental problems of geophysics and astrophysics, using the Boussinesq approximation, the acceleration vector of free fall is directed along the radius to the center of the spherical layer, and not vertically downward. Some results of a comparison of local and integral (heat exchange similarity equations) characterization of convective heat transfer for a non-conductive fluid between isothermal concentric spheres, when the acceleration vector of free fall was directed vertically down and along the radius to the center of the spherical layer, are given in [1]. This comparison showed significant differences in the heat transfer and hydrodynamics of the liquid in the layer, depending on the orientation of the acceleration vector of gravity. In this connection, an independent interest is the investigation of convective heat transfer in spherical layers, when the acceleration vector of free fall is directed along the radius to the center of the spherical layer.

2. Mathematical Model

Convective heat transfer of an electrically conductive liquid is described by a system of differential equations of magneto hydrodynamics and heat transfer, namely: motions, taking into account electromagnetic, inertial, viscous and lifting forces; energy, taking into account the heat of Joule dissipation and internal heat sources; magnetic induction and equations of continuity. The Boussinesq approximation is used.

The mathematical formulation of the problem in dimensionless form in the spherical coordinate system, taking into account the symmetry with respect to longitude, in the variables vortex – ω, the stream function – ψ, the temperature – ϑ, has the form [2]:

$$\frac{1}{Ho}\frac{\partial\omega}{\partial\tau}+\frac{1}{r^2\sin\theta}\left[\frac{\partial\psi}{\partial\theta}\frac{\partial\omega}{\partial r}-\frac{\partial\psi}{\partial r}\frac{\partial\omega}{\partial\theta}-\frac{\omega}{r}\frac{\partial\psi}{\partial\theta}+\omega\ \mathrm{ctg}\,\theta\frac{\partial\psi}{\partial r}\right]=$$

$$=\frac{1}{Re}\left[\frac{\partial^2\omega}{\partial r^2}+\frac{2}{r}\frac{\partial\omega}{\partial r}+\frac{1}{r^2}\frac{\partial^2\omega}{\partial\theta^2}+\frac{\mathrm{ctg}\,\theta}{r^2}\frac{\partial\omega}{\partial\theta}-\frac{\omega}{r^2\sin^2\theta}\right]-$$

$$-\frac{Gr}{Re^2}\frac{1}{r}\frac{\partial\vartheta}{\partial\theta}+\frac{S}{Re_m}\left[B_r\frac{\partial^2 B_\theta}{\partial r^2}+2\frac{B_r}{r}\frac{\partial B_\theta}{\partial r}+\frac{\partial B_r}{\partial r}\frac{\partial B_\theta}{\partial r}+\frac{B_\theta}{r}\frac{\partial B_r}{\partial r}-\right.$$

$$\left.-\frac{B_r}{r}\frac{\partial^2 B_r}{\partial r\partial\theta}-\frac{1}{r}\frac{\partial B_r}{\partial r}\frac{\partial B_r}{\partial\theta}+\frac{B_\theta}{r}\frac{\partial^2 B_\theta}{\partial r\partial\theta}+\frac{1}{r}\frac{\partial B_\theta}{\partial r}\frac{\partial B_\theta}{\partial\theta}+\frac{2B_\theta}{r^2}\frac{\partial B_\theta}{\partial\theta}-\frac{B_\theta}{r^2}\frac{\partial^2 B_r}{\partial\theta^2}-\frac{1}{r^2}\frac{\partial B_r}{\partial\theta}\frac{\partial B_\theta}{\partial\theta}\right];$$

$$\frac{\partial^2\psi}{\partial r^2}+\frac{1}{r^2}\frac{\partial^2\psi}{\partial\theta^2}-\frac{\mathrm{ctg}\,\theta}{r^2}\frac{\partial\psi}{\partial\theta}=-\ \omega r\sin\theta\ ;$$

$$\frac{1}{Ho}\frac{\partial\vartheta}{\partial\tau}+\frac{1}{r^2\sin\theta}\left(\frac{\partial\psi}{\partial\theta}\frac{\partial\vartheta}{\partial r}-\frac{\partial\psi}{\partial r}\frac{\partial\vartheta}{\partial\theta}\right)-\frac{1}{Pe}\left(\frac{\partial^2\vartheta}{\partial r^2}+\frac{2}{r}\frac{\partial\vartheta}{\partial r}+\frac{1}{r^2}\frac{\partial^2\vartheta}{\partial\theta^2}+\right.$$

$$\left.+\frac{\mathrm{ctg}\,\theta}{r^2}\frac{\partial\vartheta}{\partial\theta}+Q_v\right)-\frac{J}{Pe}\left(\frac{\partial B_\theta}{\partial r}+\frac{1}{r}B_\theta-\frac{1}{r}\frac{\partial B_r}{\partial\theta}\right)^2=0\ ;$$

$$\frac{1}{Ho}\frac{\partial B_r}{\partial\tau}=\frac{1}{r^2\sin\theta}\left[\frac{B_\theta}{r}\frac{\partial^2\Psi}{\partial\theta^2}+\frac{1}{r}\frac{\partial B_\theta}{\partial\theta}\frac{\partial\Psi}{\partial\theta}+B_r\frac{\partial^2\Psi}{\partial r\partial\theta}+\frac{\partial B_r}{\partial\theta}\frac{\partial\Psi}{\partial r}\right]+$$

$$+\frac{1}{Re_m}\left[\frac{\partial^2 B_r}{\partial r^2}+\frac{2}{r}\frac{\partial B_r}{\partial r}+\frac{1}{r^2}\frac{\partial^2 B_r}{\partial\theta^2}+\frac{\mathrm{ctg}\,\theta}{r^2}\frac{\partial B_r}{\partial\theta}-\frac{2B_r}{r^2}-\frac{2B_\theta\ \mathrm{ctg}\,\theta}{r^2}-\frac{2}{r^2}\frac{\partial B_\theta}{\partial\theta}\right];$$

$$\frac{1}{Ho}\frac{\partial B_\theta}{\partial\tau}=\frac{1}{r\sin\theta}\left[-B_r\frac{\partial^2\Psi}{\partial r^2}-\frac{\partial B_r}{\partial r}\frac{\partial\Psi}{\partial r}-\frac{B_\theta}{r}\frac{\partial^2\Psi}{\partial r\partial\theta}+\frac{B_\theta}{r^2}\frac{\partial\Psi}{\partial\theta}-\frac{1}{r}\frac{\partial\Psi}{\partial\theta}\frac{\partial B_\theta}{\partial r}\right]+$$

$$+\frac{1}{Re_m}\left[\frac{\partial^2 B_\theta}{\partial r^2}+\frac{2}{r}\frac{\partial B_\theta}{\partial r}+\frac{1}{r^2}\frac{\partial^2 B_\theta}{\partial\theta^2}+\frac{\mathrm{ctg}\,\theta}{r^2}\frac{\partial B_\theta}{\partial\theta}-\frac{B_\theta}{r^2\sin^2\theta}+\frac{2}{r^2}\frac{\partial B_r}{\partial\theta}\right].$$

The value of J determines the heat of Joule dissipation in the energy equation. In carrying out the computational experiment for the temperature, the following boundary conditions were set: the values of the heat flux on the inner surface of the spherical layer Γ_1 ($r = 1$) and the temperature at the outer Γ_2 ($r = r_2$):

$\left.\frac{\partial\vartheta}{\partial\theta}\right|_{\Gamma_1}=-1;\ \vartheta|_{\Gamma_2}=0$. On the axis of symmetry: $\left.\frac{\partial\vartheta}{\partial\theta}\right|_{\theta=0,\pi}=0$.

The boundary conditions for the stream function, the strength of the vortex and the magnetic induction were as follows [3]:

$$\Psi|_{\Gamma_{1,2}}=\Psi|_{\theta=0,\pi}=\omega|_{\theta=0,\pi}=0;\ \left.\frac{\partial B_r}{\partial\theta}\right|_{\theta=0,\pi}=\left.\frac{\partial B_\theta}{\partial\theta}\right|_{\theta=0,\pi}=0;$$

$$B_r|_{\Gamma_1}=B_r|_{\Gamma_2}=0;\ B_\theta|_{\Gamma_1}=-0.01\sin\theta\ ;\ B_\theta|_{\Gamma_2}=0.01\sin\theta\ .$$

The boundary conditions for the vortex at the boundaries of the layer assume a linear change in it along the normal.

The local and averaged Nusselt numbers at the boundaries of the layer were calculated by the formulas:

$$Nu_1 = -\left.\frac{\partial \vartheta}{\partial r}\right|_{\Gamma_1}, \quad Nu_2 = -r_2\left.\frac{\partial \vartheta}{\partial r}\right|_{\Gamma_2}; \quad \overline{Nu_1} = -\frac{1}{2}\int_0^{\pi}\left[\frac{\partial \vartheta}{\partial r}\right]_{\Gamma_1}\sin\theta d\theta, \quad \overline{Nu_2} = -\frac{r_2}{2}\int_0^{\pi}\left[\frac{\partial \vartheta}{\partial r}\right]_{\Gamma_2}\sin\theta d\theta.$$

The numerical solution of the problem was carried out by the finite element method; the solution algorithm is presented in [4]. The calculations were performed with the following values of the dimensionless of similarity numbers: $Re=Pe=10^2$; $Re_m=10^2$; $S=10^4$; the ratio of the inner diameter of the spherical layer to the outer diameter d / D = 1 / 2.8 (according to P. Roberts). In figure 1, 2 show the results of stationary calculations.

3. Results

In figure 1 shows the results (I – without taking into account the heat of Joule dissipation, II (Q_v = 0.2) and III (Q_v = 2), taking into account the heat of Joule dissipation and the internal heat sources Q_v) for Grashof numbers $Gr = 10^3$.

When heat of Joule dissipation is not taken into account (figure 1, I, a), heat exchange in the layer is effected by convection. The main temperature change occurs in the region of the poles and in a thin layer near the inner surface of the equatorial plane. The maximum temperature in the layer $\vartheta_{max} = 5.706$.

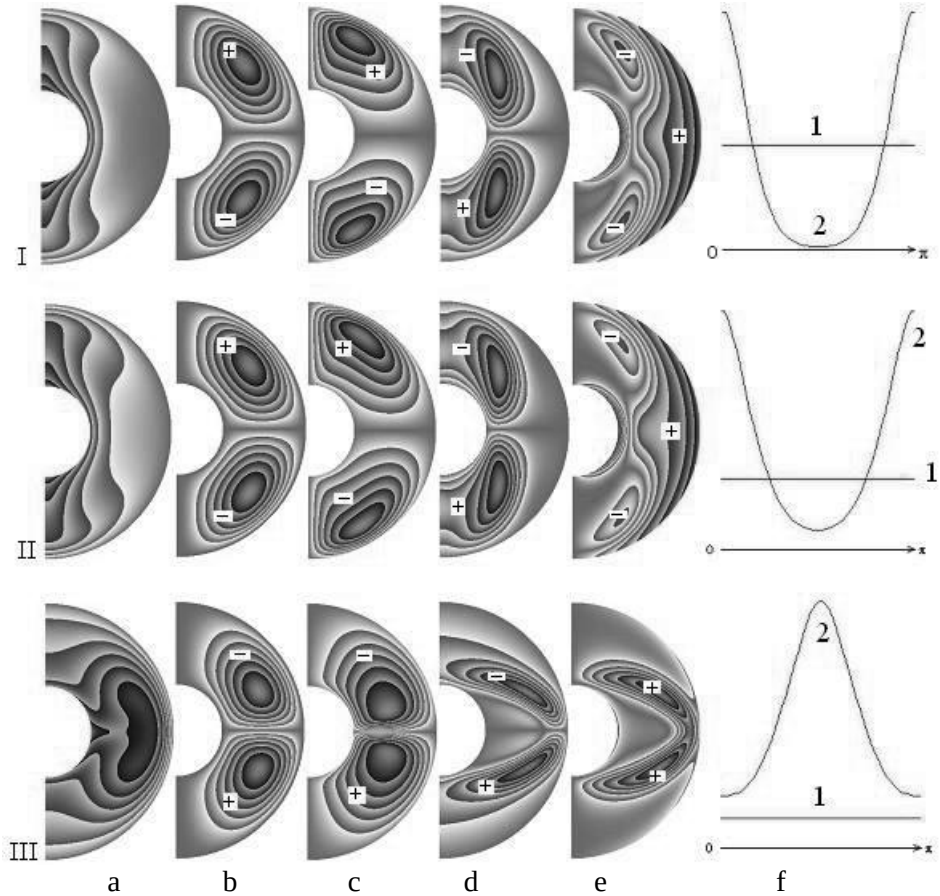

Figure 1. Calculated fields.
(a) – temperature; (b) – stream function; (c) – tension of vortex; (d, e) – radial and meridional components of magnetic induction; (f) – distribution of Nusselt numbers

The distribution of the local Nusselt numbers (figure 1, I, f) on the outer surface of the layer for $\theta \sim \pi/2$ has a minimum (on the inner surface of the layer line – 1, on the outer – 2). For the considered temperature boundary condition of the second kind on the inner surface of a spherical layer, the local and averaged Nusselt numbers on this surface assume a constant value equal to 10 for all regimes. The averaged and local Nusselt numbers on the outer surface of the layer are as follows: $\overline{Nu}_2 = 3.721$; $0.275 \le Nu_2 \le 22.758$. Heat transfer on the inner surface of the layer is more intense than on the outer surface. Two convective cells are formed in the layer (figure 1, I, b) and two vortices (figure 1, I, c). In the convective cell and the vortex of the northern hemisphere, the fluid moves counterclockwise (positive values, the sign ″+″) and the southern one - clockwise (negative values, sign″–″). Maximum values of the stream function $|\Psi| = 6.22 \cdot 10^{-2}$; of the vortex intensity $|\omega| = 3.21 \cdot 10^{-1}$. The field of the radial component of the magnetic induction (figure 1, I, d) is represented by two separate "magnetic cells" in the region of the poles, whose values ($|B_r| = 7.32 \cdot 10^{-3}$) in the northern hemisphere are negative, and in the southern hemisphere are positive. The field of the meridional component of the magnetic induction (figure 1, I, e) is represented by two connecting "magnetic cells", the values of which ($|B_\theta| = 1 \cdot 10^{-2}$) in the northern hemisphere are negative, and in the southern hemisphere are positive. In the rest of the region, they are positive at the outer surface and negative at the inner surface.

Allowance for the heat of Joule dissipation and internal heat sources with a power $Q_v = 0.2$ (figure 1, II) leads to insignificant changes in the calculated fields in comparison with the results of figure 1, I. The maximum value of the temperature in the layer $\vartheta_{max} = 6.410$. The averaged and local Nusselt numbers on the outer surface of the layer: $\overline{Nu}_2 = 8.668$; $2.760 \le Nu_2 \le 33.632$. $|\Psi| = 8.03 \cdot 10^{-2}$; $|\omega| = 3.53 \cdot 10^{-1}$; $|B_r| = 4.83 \cdot 10^{-3}$; $|B_\theta| = 10^{-2}$.

The increase in the power of internal heat sources to $Q_v = 2$ (figure 1, III) leads to significant changes in the calculated fields in comparison with the results shown in figure 1, I and 1, II. The temperature field (figure 1, III, a) and the distribution of the local Nusselt numbers (figure 1, III, f) are reconstructed. A significant change in temperature occurs in the equatorial region, and its field resembles the "auricle" in shape. The maximum temperature in the layer $\vartheta_{max} = 9.036$. The intensity of heat exchange on the outer surface of the layer becomes is more significant than on the inside. The structure of the fluid flow changes. It turned out that for this regime the direction of the fluid in the cells and vortices changes (figure 1, III, b, c) by the opposite direction as compared with the results shown in figure 1, I and 2, II, b, c. $|\Psi| = 1.88 \cdot 10^{-1}$; $|\omega| = 5.77 \cdot 10^{-1}$. The fields of the radial and meridional components of the magnetic induction (figure 1, III, d, e) underwent significant changes in comparison with the results shown in figure 1, I and 1, II, d, e. $|B_r| = 3.47 \cdot 10^{-2}$; $|B_\theta| \in [-10^{-2}; 4.58 \cdot 10^{-2}]$.

In figure 2 shows similar results for Grashof numbers $Gr = 10^4$.

When heat of Joule dissipation is not taken into account (figure 2, I, a), heat exchange in the layer is carried out by convection. The main temperature change occurs in the region of the poles and in a narrow layer of the equatorial plane. The distribution of the local Nusselt numbers (figure 2, I, f) on the outer surface of the layer has two minima, and for $\theta \sim \pi/2$ one maximum. Heat transfer on the inner surface of the layer is more intense than on the outer surface. The maximum temperature in the layer $\vartheta_{max} = 3.344$. The averaged and local Nusselt numbers on the outer surface of the layer: $\overline{Nu}_2 = 3.670$; $0.214 \le Nu_2 \le 9.194$. Two convective cells are formed in the layer (figure 2, I, b) and four vortices (figure 2, I, c). In a convective cell and a large-scale vortex of the northern hemisphere, the liquid moves clockwise, and the southern one – against. The maximum values of the stream function are $|\Psi| = 2.34 \cdot 10^{-2}$; the intensity of the vortex is $|\omega| = 9.70 \cdot 10^{-1}$. The field of the radial constituent magnet-

ic induction (figure 2, I, d) is represented by two separate "magnetic cells", whose values ($|B_r| = 1.48$) in the northern hemisphere are positive, and in the southern hemisphere are negative.

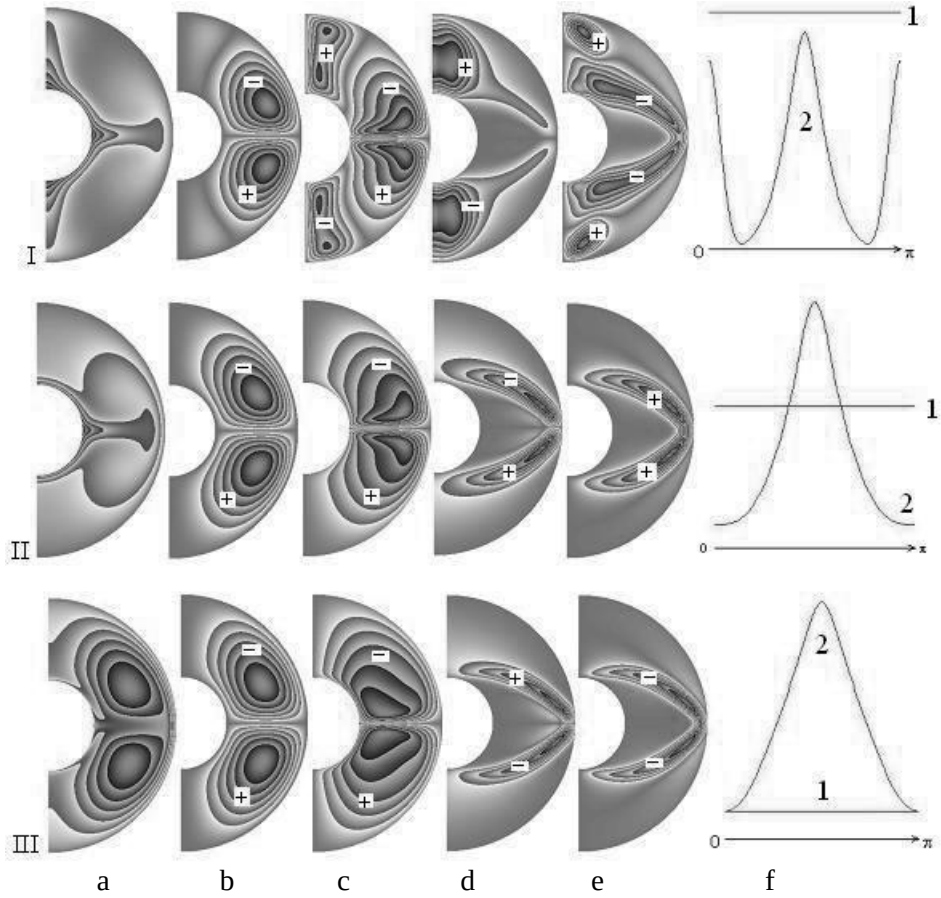

Figure 2. Calculated fields.
(a) – temperature; (b) – stream function; (c) – tension of vortex; (d, e) – radial and meridional components of magnetic induction; (f) – distribution of Nusselt numbers

The field of the meridional component of the magnetic induction (figure 2, I, e) is represented by four "magnetic cells": two connected in the main region and two small-scale in the region of the poles.

Allowance for the heat of Joule dissipation and internal heat sources of power $Q_v = 0.2$ (figure 2, II) leads to significant changes in the calculated fields in comparison with the results of figure 2, I. A significant change in the temperature field occurs in the region of the equator, resembling the "fungus" in shape. Maximum value of temperature in the layer $\vartheta_{max} = 3.179$. The distribution of the local Nusselt numbers (figure 2, II, f) on the outer surface of the layer for $\theta \sim \pi/2$ has a maximum. The averaged and local Nusselt numbers on the outer surface of the layer: $\overline{Nu}_2 = 8.667$; $1.598 \le Nu_2 \le 17.206$. Heat transfer on the inner surface of the layer is more intense than on the outer surface. $|\Psi| = 3.15 \cdot 10^{-1}$; $|\omega| = 1.10$; $|B_r| = 1.06$; $|B_\theta| \in [-6.83 \cdot 10^{-2}; 1.37]$.

The increase in the power of internal heat sources to $Q_v = 2$ (figure 2, III) leads to changes in the calculated fields in comparison with the results presented in figure 1, I and 1, II. The temperature field (figure 2, III, a) and the distribution of the local Nusselt numbers (figure 2, III, f) are reconstructed. Maximum value of temperature in the layer $\vartheta_{max} = 6.900$. The averaged and local Nusselt numbers on the outer surface of the

layer are: $\overline{Nu}_2 = 53.267$; $10.035 \le Nu_2 \le 85.722$. The intensity of heat exchange on the outer surface of the layer becomes more significant than on the inner surface. $|\Psi| = 5.96 \cdot 10^{-1}$; $|\omega| = 1.98$; $|B_r| = 4.07$; $|B_\theta| \in [-5.06; 4.21 \cdot 10^{-1}]$.

4. Conclusion

Analysis of the results obtained allows us to draw the following conclusions:

1. The joint influence of the heat of Joule dissipation and internal heat sources on the heat exchange and magneto hydrodynamic structure of the flow of an electrically conductive liquid in a spherical layer is investigated;

2. For the Grashof number $Gr = 10^3$, when the heat of Joule dissipation is taken into account and $Q_v = 2$, there is a significant change in the temperature and magnetic induction fields. In this case, the direction of fluid motion in convective cells and vortices is reversed in comparison with the results of other cases of this regime.

3. An increase in the Grashof number to 10^4 leads to significant changes in all calculated fields, both with allowance for the heat of Joule dissipation ($Q_v = 0.2$; 2) and without it. For all considered regimes, the heat exchange in the layer is carried out by convection, the structure of the liquid flow changes, "magnetic cells" are formed in the field of the radial component of the magnetic induction;

4. For the Grashof number $Gr = 10^4$ without taking into account the heat of Joule dissipation, in comparison with the results of figure 1, the magnetic poles change (from north to south and from south to north). This phenomenon periodically occurs in the life of the Earth;

5. The mathematical model and the results obtained can be useful in modeling thermal and magneto hydrodynamic processes in the liquid core of the Earth and other planets.

5. References

[1] S. Solovjov 2017 Simulation of heat exchange in the liquid core of the Earth *Journal of Engineering Physics and Thermophysics* vol 90 4 pp 873-882

[2] S. Solovjov 2017 Influence of joule dissipation on heat exchange and magnetic hydrodynamics of liquid in a spherical layer. Part I *Journal of Engineering Physics and Thermophysics* vol 90 5 pp 1251-1265

[3] S. Solovjov 2015 Heat transfer modeling of an electrically conducting fluid in a spherical layer *Numerical Analysis and Applications* vol 88 4 pp 351-364

[4] S. Solovjov 2015 Simulation of Convective Heat Exchange in the Electrically Conducting Liquid in a Spherical Cavity. Algorithm of Solution *Journal of Engineering Physics and Thermophysics* vol 88 6 pp 1416-1431